applied sciences

MDPI

Article

Hybrid Ionic Liquid–Silica Xerogels Applied in CO_2 Capture

Aline S. Aquino [1], Michele O. Vieira [2], Ana Sofia D. Ferreira [3], Eurico J. Cabrita [3,*], Sandra Einloft [2] and Michèle O. de Souza [1,*]

1 Universidade Federal do Rio Grande do Sul (UFRGS), Avenida Bento Gonçalves, 9500. 91501-970 Porto Alegre/RS, Brazil
2 Pontifícia Universidade Católica do Rio Grande do Sul (PUCRS), Avenida Ipiranga, 6681. 90619-900 Porto Alegre/RS, Brazil
3 UCIBIO, Faculdade de Ciências e Tecnologia, Universidade Nova de Lisboa (FCT-UNL), Campus da Caparica. 2829-516 Caparica, Portugal
* Correspondence: ejc@fct.unl.pt (E.J.C.); michele.souza@ufrgs.br (M.O.d.S.); Tel.: +55-51-3308-7238 (M.O.S.)

Received: 30 April 2019; Accepted: 26 June 2019; Published: 28 June 2019

Abstract: The imidazolium-based ionic liquids (ILs) are solvents known for selectively solubilizing CO_2 from a gas CH_4/CO_2 mixture, hence we have produced new hybrid adsorbents by immobilizing two ILs on xerogel silica to obtain a solid–gas system that benefits the ILs' properties and can be industrially applied in CO_2 capture. In this work, the ILs $(MeO)_3$Sipmim.Cl and $(MeO)_3$Sipmim.Tf_2N were used at different loadings via the sol–gel process employing a based 1-methyl-3-(3-trimethoxysylilpropyl) imidazolium IL associated to the anion Cl^- or Tf_2N^- as a reactant in the synthesis of silica xerogel. The CO_2 adsorption measurements were conducted through pressure and temperature gravimetric analysis (PTGA) using a microbalance. SEM microscopies images have shown that there is an IL limit concentration that can be immobilized (ca. 20%) and that the xerogel particles have a spherical shape with an average size of 20 µm. The adsorbent with 20% IL $(MeO)_3$Sipmim.Cl, SILCLX20, shows greater capacity to absorb CO_2, reaching a value of 0.35 g CO_2/g adsorbent at 0.1 MPa (298 K). Surprisingly, the result for xerogel with IL $(MeO)_3$Sipmim.Tf_2N shows poor performance, with only 0.05 g CO_2/g absorbed, even having a hydrophobic character which would benefit their interaction with CO_2. However, this hydrophobicity could interfere negatively in the xerogel synthesis process. The immobilization of ionic liquids in silica xerogel is an advantageous technique that reduces costs in the use of ILs as they can be used in smaller quantities and can be recycled after CO_2 desorption.

Keywords: carbon dioxide; imidazolium ionic liquids; immobilization; xerogel; silica

1. Introduction

Excessive increase in greenhouse gas concentrations, especially carbon dioxide, stems from an energetic matrix based on the combustion of fossil fuels which causes global warming and has other environment impacts [1–3]. Mitigation of these impacts has been the subject of research for the development of adsorbents for CO_2 capture by the application of carbon capture and storage (CCS) or carbon capture utilization (CCU) technologies [4–8].

Ionic liquids (ILs) ionic liquids are a class of materials widely studied in recent times. It has been proposed as an alternative solvent for CCS or conversion [9–15]. These solvents are selective for CO_2 separation in CO_2/CH_4 gas mixtures [16,17]. As the ILs are non-volatile compounds, when CO_2 is desorbed under depressurized conditions, no loss of solvent occurs. Moreover, one can design the

chemical structure of ILs, choosing the appropriate cation/anion to optimize the capacity of the ionic liquid in the CO_2 absorption [18–21].

Incorporating ILs in solid matrices emerged as a new and challenging field, allowing the use of heterogeneous systems for CO_2 capture [22–25]. The immobilization process is usually carried out by cationic or anionic incorporation, or by cationic anchorage, or through in-situ polymerization via a sol–gel process [26,27]. In the case of cationic or anionic incorporation, the IL is synthesized and then fixed into the inorganic material through an IL cation or anion anchorage. In the case of the in situ polymerization via sol–gel process, the IL is used as a templating agent for the synthesis of silica xerogels due to its surfactant character and the low surface tension which enables control of the silica particle size, gelation time, structures, and morphology [28,29].

In the classical sol–gel process, an alkoxide precursor is hydrolyzed leading to the formation of Si-OH bonds (silanol groups) that condensate forming an inorganic three-dimensional network. The targeted material is then obtained after drying—xerogel or aerogel [30].

The IL acts like a solvent, catalyst or template in in-situ polymerization, bringing with it the advantage of being easier to handle and having wider applicability in various fields. ILs improve the efficiency and selectivity and allow easy separation of the products and catalyst recycle, especially in catalysis [31,32].

With the immobilization of ILs in gels leading to ionogels, these materials are applied in electrochemistry devices to encapsulate functional molecules (catalysts, sensing molecules, fluorescent metal complexes) offering a new method to functionalize nanostructured inorganic materials [33,34]. The xerogel silica final structure is highly influenced by the nature of the alkyl-alkoxysilanes precursor such as the chain length, functionality, and its hydrophobic character. These properties can be modified adding a wide range of compounds to the alkyl-alkoxysilanes precursor, such as surfactants like ionic liquids [35].

The combination of the well-known affinity between pure ILs and CO_2 [9,11,16–19] and solid adsorbents leads to a synergic effect reported by Aquino et al. [25]. Therefore, this study aims to synthesize hybrid silica–IL xerogels via a sol–gel process using different alkyl-alkoxysilanes compounds: the tetramethoxysilane (TMOS), the methyltrimetoxysilane (MTMS), and a based 1-methyl-3-(3-trimethoxysylilpropyl) imidazolium IL associated to the anion Cl^- or Tf_2N^- incorporated in the range 1–40% IL/ alkyl-alkoxysilanes v/v. During the synthesis, TMOS and MTMS are hydrolyzed leading to the formation of silanols groups. Part of these silanol groups condensate producing a three-dimensional network and the remaining silanol groups will react with the IL ensuring its participation in the structure building.

These materials were evaluated for CO_2 adsorption. It is important to highlight that the use of IL as a precursor for the synthesis of xerogel is an innovative route for increasing the CO_2 adsorption of the material. The IL is responsible for the three-dimensional matrix formation as well as for increasing the affinity between the CO_2 and the adsorbent. Typical CO_2 adsorption values are approximately 0.09 g per g of neat ionic liquid [20].

2. Materials and Methods

2.1. Chemicals

Lithium bis(trifluoromethylsulfonyl) imide ($LiTf_2N$) (Alfa Aesar, 98.0%); (3-chloropropyl)trimethoxysilane (Alfa Aesar, 97.0%); sodium fluoride (NaF) (Sigma Aldrich, 99.0%); 1-methylimidazole (Sigma Aldrich, 99.5%); tetramethoxysilane (TMOS) (Sigma Aldrich, 98.5%); polyvinyl alcohol (PVA; Mn 15.000) (Sigma Aldrich, 88.0%); methyltrimetoxysilane (MTMS) (Sigma Aldrich, 98.5%); carbon dioxide (CO_2) (Air Liquide, 99.998%).

2.2. Ionic Liquid Synthesis

Firstly, 1-methyl-3-(3-trimethoxysilylpropyl) imidazolium chloride was synthesized through the reaction of 1-methylimidazole with (3-chloropropyl) trimethoxysilane (molar ratio 1: 1.5) at 363 K for 48 h. Then the reaction mixture was cooled down to room temperature and the organic upper phase separated. The resulting product was a yellow viscous ionic liquid. Then the IL phase was washed thoroughly with diethyl ether and residual ether was removed under vacuum.

An equimolar amount of $LiTf_2N$ was added to a solution of $(MeO)_3$Sipmim.Cl in dry acetone and left under stirring for five days at room temperature. After concentrating under vacuum, the solid was solubilized in dichloromethane, dried, filtered over a celite bed, and washed with water until $AgNO_3$ test was negative. The organic phase was dried over anhydrous $MgSO_4$, filtrated and the solvent was removed under vacuum [36–38]. The structure of the ILs $(MeO)_3$Sipmim.Cl and $(MeO)_3$Sipmim.Tf_2N and was confirmed by ^{1}H-NMR and FTIR.

$(MeO)_3$Sipmim.Cl: ^{1}H-NMR (400 MHz, $CDCl_3$, 298 K) δ (ppm): 0.58 (m, CH_2Si); 1.91 (m, CH_2CH_2N); 3.49 (s, $SiOCH_3$); 3.63 (s, CH_3N); 4.06 (t, CH_2N); 4.27 (t, CH_2); 7.39 (s, H5); 7.61 (s, H4); 10.39 (s, H2). FTIR ν (cm^{-1}): 3031, Si-O; 2944-2839 for aliphatic C-H stretching (methyl and methylene groups); 1570-1457 C=C stretching and C-N of the imidazolium ring; 1175-1071 Si-OCH_3; 805 from Cl^- anion.

$(MeO)_3$Sipmim.Tf_2N: ^{1}H-NMR (400 MHz, $CDCl_3$, 298 K) δ (ppm): 0.51 (m, CH_2Si); 1.85 (m, CH_2CH_2N); 3.47 (s, $SiOCH_3$); 3.83 (s, CH_3N); 4.25 (t, CH_2N); 7.70 (s, H5); 7.61 (s, H4); 8.99 (s, H2). FTIR ν (cm^{-1}): 3161-3115, Si-O; 2934-2853 for aliphatic C-H stretching (methyl and methylene groups); 1572-1460 C=C stretching and C-N of the imidazolium ring; 1182-1047 Si-OCH_3; 791-742 from Tf_2N^- anion.

2.3. Ionic Liquid Immobilization

The IL was dissolved in an aqueous solution containing NaF (0.20 g L^{-1}) and PVA (4.64 g L^{-1}). The amount of water in this solution was fixed (6.86 mmol). The solution was vigorously shaken on a vortex mixer. The precursors were then added (Figure 1) in amounts that yielded a water/silane molar ratio of 1:8, irrespective of the type and number of precursors used (e.g., 0.143 mmol of TMOS and 0.714 mmol MTMS in 1:5 TMOS/MTMS gels).

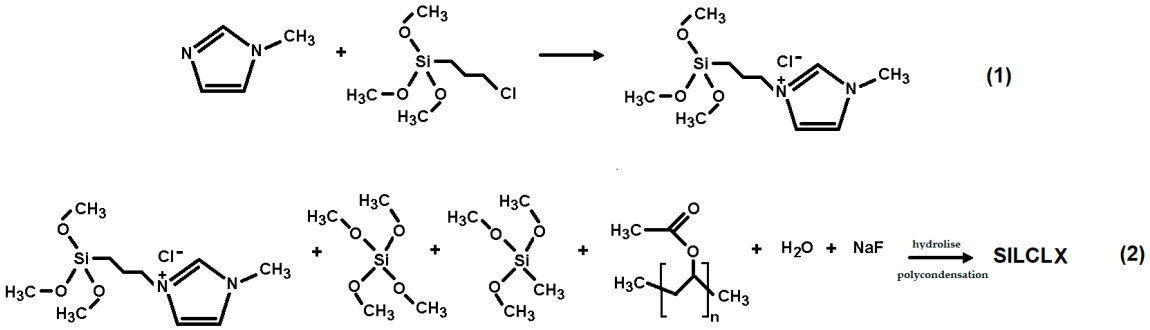

Figure 1. Ionic liquid synthesis (1) and immobilization by sol–gel method (SILCLX) (2).

The % (v/v) of IL (1, 5, 10, 20, 30, and 40%) was determined by the IL volumes and the total volume of the solution containing water, NaF, PVA, TMOS, and MTMS.

The mixture was again vigorously shaken on the vortex mixer until it became homogeneous. It was then placed in an ice bath until gelation occurred (after a few seconds), and kept in the ice bath for an additional 10 min. The container with the obtained gel was kept at 277 K for 24 h, after which the gel was put in a kiln at 308 K for 24 h. The white gel obtained was crushed and washed (for about 10 min)/centrifuged (at 10,000 rpm), first using acetone then n-pentane (also 2 mL of each). The gel was left at 308 K for 24 h in a kiln [34].

The obtained samples were denominated according to the IL content and the anion present as described as supported ionic liquid (SIL)-Anion (TF2N or CL for $(MeO)_3$Sipmim.Tf_2N and $(MeO)_3$Sipmim.Cl respectively)–Xerogel (X)–% IL (number corresponding to the % of loaded IL)).

2.4. Characterization

The FTIR spectra were collected on a PerkinElmer Spectrum 100 spectrometer in KBr pellet form. NMR measurements were performed at room temperature using a Bruker Avance III 400 MHz spectrometer; solid-state NMR cross-polarization magic angle spinning (^{29}Si CPMAS) at 5 kHz was selected to record silicon spectra. SEM on Microscope Analytical JEOL, model 7001F FEG-SEM. The surface area and pore size were calculated from sorption analyses (N_2 at 77 K) using a Micromeritics Instrument Corporation, TriStar II 3020 V1.03 and Brunauer–Emmett–Teller (BET) method. The real density of xerogel samples (ρs) was determined on Ultrapycnometer 1000—Quantachrome Corporation, cell volume of 20.45 cm^3, and pressure of 21.0 psi (1.45 bar).

2.5. CO_2 Adsorption Measurements

The sorption of CO_2 in the samples were gravimetrically assessed in a magnetic suspension balance (MSB), (Rubotherm Prazisionsmesstechnik GmbH, 35 MPa and 673 K) equipped with a single sinker device for adsorbate density determination and thermostatized with an oil bath (Julabo F25/± 273 K). The apparatus details are well described elsewhere. When compared to other gravimetrical sorption methods, the MSB device has the advantage of allowing high-pressure sorption measurements as the sample can be potted into a closed chamber coupled to an external precise balance (accuracy of ±10 μg).

The samples (0.06 to 0.09 g) were weighed and transferred to the MSB sample container, and the system was subjected to a 10^{-7} MPa vacuum at the temperature of the sorption measurement, 298 K, for 24 h (constant weight was achieved in this time). The CO_2 was admitted into the MSB pressure chamber up to the desired pressure, 0.1–2 MPa in this study, a pressure gauge with an accuracy of 10^{-3} MPa was used to control the system pressure.

The solubility of CO_2 in the samples for each isotherm and pressure considered was measured 3–4 hours after no more weight increasing for CO_2 sorption had been observed. At this step of CO_2 solubility in the samples, the weight reading from the microbalance at pressure P and temperature T is recorded as $W_t(P,T)$. The mass of dissolved CO_2 in the sample $(W_{absolute})$ was calculated using Equation (1)

$$W_{absolute} = \left[W_t(P,T) - W_{sc}(P,T) + \rho_g(P,T)\cdot(V_{sc}(T) + V_s(T) + V_{ads})\right] - W_s(vac,T) \quad (1)$$

where $W_{sc}(P,T)$ is the weight of sample container, $\rho_g(P,T)$ stands for CO_2 density, directly measured with the MSB coupled single-sinker device, $V_{sc}(T)$ is the volume of the sample container, determined from a buoyancy experiment when no sample is charged into the sample container, $V_s(T)$ the specific solid sample volume, $W_s(vac,T)$ is the weight of samples under vacuum and the term $\rho_g(P,T)\cdot(V_{sc}(T) + V_s(T))$, represents the buoyancy force.

The volume of the adsorbed phase V_{ads} must be taken into account in the buoyancy correction to determine the absolute gas adsorption. In this paper, the density of the adsorbed phase ρ_{ads} was assumed to be the density of liquid CO_2 in a reference state (boiling point at 1 atm) and the V_{ads} was obtained by dividing the adsorbed mass, m_{ads} by the density of the adsorbed phase, ρ_{ads}. Further details on data handling from the adsorption isotherms measured may be found in literature [39,40].

3. Results

The FTIR spectra of the xerogel matrix and SILTF2NX20 (see Figure A1), respectively, show i) in the region between 3550–3416 and 3488 cm^{-1} the presence of O-H bands of silanol groups; ii) at 2977 and 2975 cm^{-1} C-H stretching of CH_3 groups; and iii) at 1638 and 1627 cm^{-1} C-O stretching of

methoxy groups. In these spectra, the presence of bands 1277 and 1275 cm^{-1} characterize the Si-CH_3 bond and at 1037 and 1049 cm^{-1} the Si-O-Si bond. The presence of the imidazole IL linked to the xerogel is mainly characterized by a band at 1577 cm^{-1} corresponding to a C=C aromatic stretching and a band at 3167 cm^{-1} corresponding to an aromatic C-H, both belonging to the imidazolium ring [37,41]. In addition, the FTIR spectrum of SILTF2NX20 also shows two signals at 1353 and 1196 cm^{-1} corresponding respectively to the Si-O and Si-O-CH_3 stretching [37].

It is noteworthy that the siloxane bands of Si-O-Si, in the range of 1136–1186 cm^{-1} and disiloxane band of R_3Si-O-SiR_3 in the range of 1049–1070 cm^{-1} are ascribed to the chemical bonds between silicon and IL indicating a strong interaction between the IL and the gel matrix.

Table 1 presents data corresponding to the ^{29}Si CPMAS analysis of the xerogel matrix synthesized without IL, XEROGEL, and the xerogel containing IL. This data confirms, in the case of XEROGEL, the presence of chemical environments for Si at −63.58 and −72.38 ppm related to T^2 and T^3, and at −117.31 ppm attributed to Q^4, respectively. For all samples containing ILs, the largest composition is of T^2 corresponding to (-O-)$_2$Si-(O-R)$_2$, independently of the anion.

Table 1. ^{29}Si CPMAS results for supported ILs in xerogel matrix.

	XEROGEL			SILCLX10			SILCLX40			SILTF2NX10			SILTF2NX40		
Form	**δ (ppm)**	**intgr**	**%**	**δ (ppm)**	**intgr**	**%**	**δ (ppm)**	**intgr**	**%**	**δ (ppm)**	**intgr**	**%**	**δ (ppm)**	**intgr**	**%**
Q2	/	/	/	/	/	/	/	/	/	/	/	/	/	/	/
Q3	/	/	/	−101.14	0.02	1.74	−102.28	0.02	1.47	/	/	/	/	/	/
Q4	−117.31	0.49	11.86	−110.21	0.13	11.30	−111.47	0.10	7.35	−110.41	0.13	10.48	−110.56	1.00	14.25
T2	−72.38	2.64	63.92	−66.06	1.00	86.96	−66.68	1.00	73.53	−66.03	1.00	80.56	−65.65	5.09	72.51
T3	−63.58	1.00	24.21	/	/	/	−58.10	0.24	17.65	−56.10	0.11	8.87	−56.49	0.93	13.25

Only the samples with the IL have the Cl^- anion present Q^3 form corresponding to (-O-)$_3$Si-OH. The forms T^2 and T^3 indicate the immobilization of IL, therefore we observed that the major quantity of T^2+T^3 is that with a higher load IL (40%). The values of T^2 and T^3 allow verification if there are free OH groups on the support or if the IL is bonded through the OH groups and then being part of the xerogel.

SEM images of the xerogel matrix and of the xerogels containing the (MeO)$_3$Sipmim.Tf_2N in different concentrations are represented in Figure 2. Based on these images it can be observed that the use of 1% IL (MeO)$_3$Sipmim.Tf_2N as precursor is not sufficient to form the typical spheres of the xerogel matrix. However, as the concentration of IL increases to 5, 10, and 20% the formation of the microspheres becomes increasingly visible. When the IL load reaches 30%, the collapse of the spheres can be observed indicating an over concentration of IL as precursor for the synthesis of the xerogel.

The images of the synthesized xerogel also demonstrate a peculiar feature related to the presence of the ionic liquids that acts as a surfactant resulting in the formation of spherical particles during the sol–gel process. As the (MeO)$_3$Sipmim.Cl and (MeO)$_3$Sipmim.Tf_2N ILs are amphiphilic structures composed of a polar head (the imidazolium ring) that is hydrophilic and carbon or siloxane chain that is hydrophobic, they form micelles during the sol–gel process synthesis [42].

The XEROGEL, SILTF2NX20, and SILTF2NX40 were characterized through N_2 sorption at 77 K and helium pycnometry. Specific surface area (S_{BET}), pore volume (V_p), pore and diameter size and density results are shown in Table 2.

Table 2. Structural properties for ILs in xerogel silica

Samples	S_{BET} (m^2/g)	V_p (cm^3/g)	Pore Size (nm) [a]	Diameter (nm) [b]	ρ_s (g/cm^3) [c]
XEROGEL	9	0.016	7.1	8.2	1.80
SILTF2NX20	4	0.008	7.5	10.2	3.08
SILTF2NX40	1	0.002	4.9	5.6	—

[a] Adsorption average pore width (by BET). [b] BJH adsorption average pore diameter. [c] Determined by helium pycnometer.

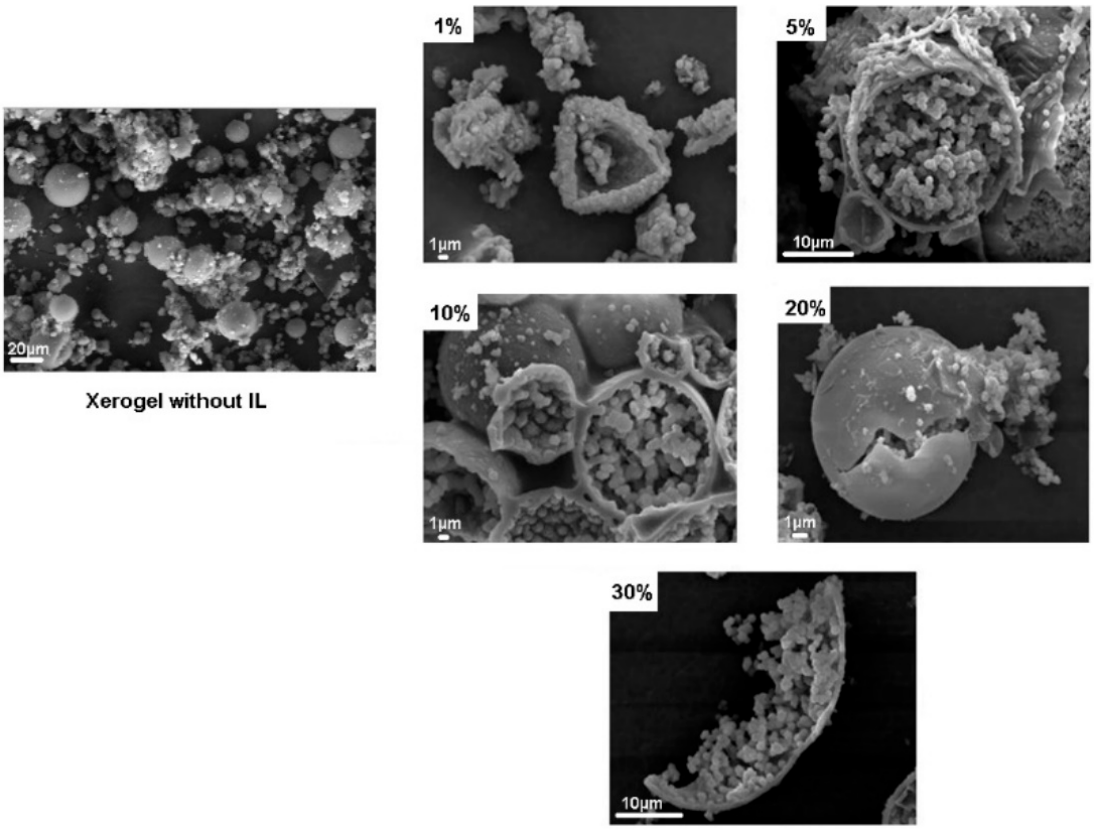

Figure 2. SEM (x 3000)—spheres of ionic liquids $(MeO)_3$Sipmim.Tf_2N in xerogel matrix.

Data obtained from N_2 sorption ($S_{BET,}$ V_p) shows that partially replacing MTMS with the IL decreases the specific surface area and the pore volume indicating that the support is more compact according to the density values.

CO_2 adsorption tests were performed immediately after the synthesis of the materials. The tested materials were the Xerogel, SILTF2NX20, SILCLX20, and SILCLX40. It is worth noting that for the calculation of the adsorption in excess and absolute from the PTGA data, the density value for the sample SILTF2NX20 obtained through helium pycnometry (see Table 2) was used. As the experimental CO_2 adsorption curves, absolute and in excess, were very similar due to employing the low working pressure, only the absolute adsorption data is presented Figure 3 as a function of CO_2 pressure.

It is evident that the sample SILCLX20 exhibits the greater capacity to CO_2 adsorption, reaching a value of 0.35 g CO_2/g adsorbent at 1.0 MPa. The sample with the same IL, but with greater immobilized concentration SILCLX40 has a very low performance, only 0.07 g CO_2/g adsorbent at the same pressure, which indicates that increasing the amount of IL immobilized in the xerogel hinders the adsorption capacity. This effect can be caused by both a block of the solid's pores by the IL and IL trapped without accessibility or free volume to adsorb CO_2.

Surprisingly, the adsorption result obtained for SILTF2NX20 (0.05 g CO_2/g adsorbent at 1.0 MPa) is very low. As the Tf_2N^- anion has a hydrophobic character, it was expected that it would improve the IL–CO_2 interaction. This result can be attributed to a low IL interaction with the xerogel silica networking.

The concentration of IL immobilized in the support as mentioned earlier has a slight adverse effect on adsorption efficiency, as the higher the concentration of IL support, the lower the mass of CO_2 adsorbed. Results obtained with SILCLX20 were distinguished from all the others and is an exceptional mark.

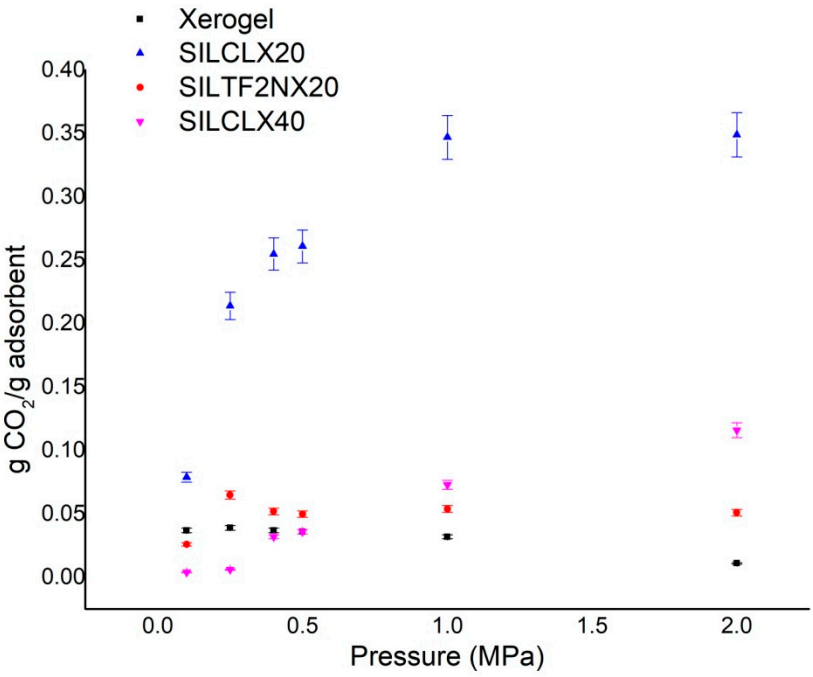

Figure 3. CO_2 adsorption at 298 K.

4. Discussion

The CO_2 sorption capacity was previously studied by Aquino et al. [25] through the same gravimetrical sorption methods and experimental conditions using mesoporous material MCM-41 (M) containing supported ionic liquids (SIL) with 50% load (50). The ionic liquids had the same $(MeO)_3$Sipmim cation and four different anions (Cl^- (CL), BF_4^- (BF4), PF_6^- (PF6), and TF_2N^- (TF2N)). This study evaluated the influence of the anion nature on the CO_2 sorption capacity (see Figure 4).

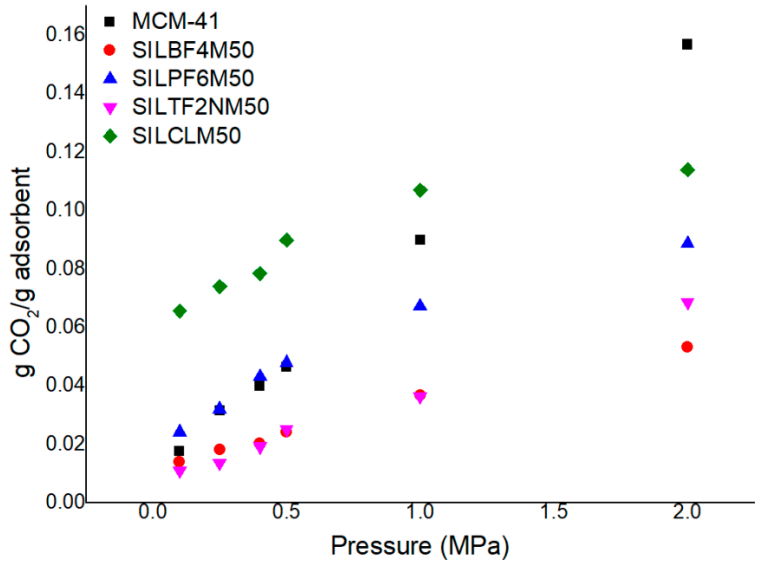

Figure 4. CO_2 adsorption in IL supported in MCM-41 at 298 K [25].

The results represented in Figure 4 clearly show that the IL containing a chloride anion (SILCLM50) had better CO_2 adsorption. For comparison, SILCLX20 (xerogel process) from our study (see Figure 3) presents a greater capacity to adsorb CO_2, reaching a value of 0.35 g CO_2/g adsorbent (at 1.0 MPa) than SILCLM50 (supported on MCM-41) which attains only 0.11 g CO_2 /g adsorbent (at 1.0 MPa) (see Figure 4). In any case, supported ILs (in xerogel or MCM-41) provide higher CO_2 adsorption capacity than when used as solvents due to the contribution of the support. The comparison of the results reported in Figures 3 and 4 indicates clearly that when using xerogel support a lower amount of IL (20%) (see Figure 3) is required than when MCM-41(50%) is employed.

Additionally, the literature reports results that described the use of different materials, such as Zeolite 13X at 303 K [43], β-zeolite at 303 K [44], and MCM-41 at 298 K [25]. The best result obtained was by Jadhav, P.D., using the zeolite 13X, 0.0550 g CO_2 being adsorbed per g of adsorbent. The addition of amine, that has an affinity with CO_2 [5] to the zeolite does not increase the quantity of CO_2 adsorbed.

The best CO_2 adsorption amount obtained in this study (SILCLX20: 0.35 g CO_2/g adsorbent) is approximatively 500 and 200% higher than when the zeolite 13X and $(MeO)_3$Sipmim.Cl supported in (MCM-41 (SILCLM50, see Figure 4) are used as an adsorbent, respectively.

After the CO_2 adsorption, the PTGA was depressurized without heating. It was verified that the sample weight remains equal to its value before the CO_2 adsorption process. This result indicates that CO_2 was physically adsorbed, and that the adsorbent material was not modified during the adsorption experiments enabling its recovery.

The higher thermal stability of the hybrid material and the possibility of their reuse in physical separation systems are properties that indicate these materials have the potential for CO_2 capture.

5. Conclusions

The sol–gel immobilization of ionic liquids is an advantageous technique that reduces costs in the use of ILs, as they can be used in smaller quantities. When ILs $(MeO)_3$Sipmim.Cl and $(MeO)_3$Sipmim.Tf_2N were supported at different concentrations of IL via the sol–gel process it was noted that there is an ideal IL concentration that can be immobilized in this matrix type (ca. 20%). The CO_2 adsorption capacity results show that these materials can be applied as adsorbents in a capture system, as they offer satisfactory CO_2 sorption capacity, the best result being obtained by SILCLX20 that reached 0.35 g CO_2/g adsorbent at 1.0 MPa pressure.

Author Contributions: The authors worked together in a doctoral research conducted in international co-tutelage. Conceptualization, E.J.C. and S.E.; Methodology, formal analysis, and investigation, A.S.A., A.S.D.F., and M.O.V.; Writing—original draft preparation, A.S.A. and M.O.V.; Writing—review and editing, S.E. and M.O.d.S.

Funding: This research was funded by CAPES Foundation, Ministry of Education of Brazil, process number 9259120 for doctoral.

Acknowledgments: We thank the Portuguese National NMR Facility (FCT-UNL and CICECO-Aveiro Institute of Materials), supported by Fundação para a Ciência e a Tecnologia (ROTEIRO/0031/2013 - PINFRA/22161/2016) (co-financed by FEDER through COMPETE 2020, POCI, and PORL and FCT through PIDDAC for NMR experiments and MicroLab – Electron Microscopy Laboratory (IST, University of Lisbon) for SEM Analysis.

Conflicts of Interest: The authors declare no conflict of interest.

Appendix A

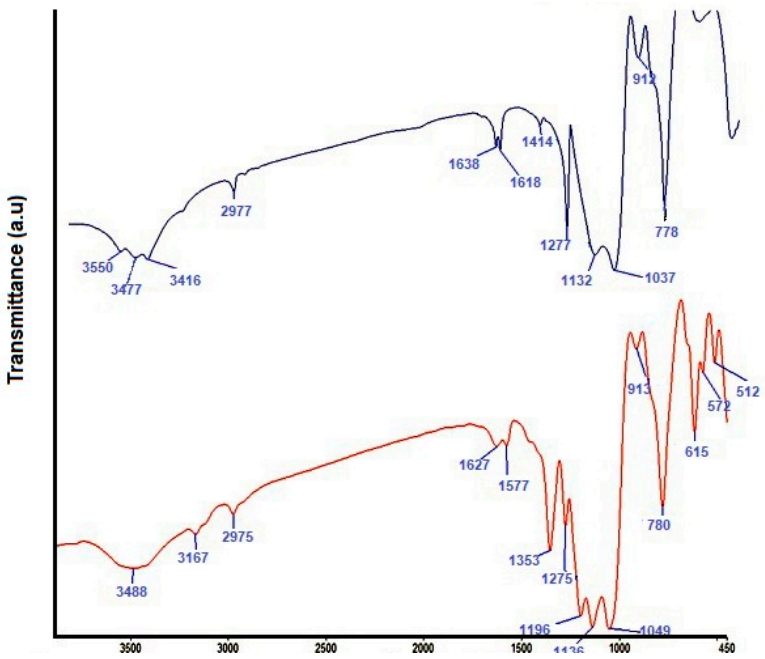

Figure A1. FTIR spectra of xerogel matrix and SILTF2NX20.

References

1. Koytsoumpa, E.I.; Bergins, C.; Kakaras, E. The CO_2 economy: Review of CO_2 capture and reuse technologies. *J. Supercrit. Fluids* **2018**, *132*, 3–16. [CrossRef]
2. Rogelj, J.D.; Shindell, K.; Jiang, S.; Fifita, P.; Forster, V.; Ginzburg, C.; Handa, H.; Kheshgi, S.; Kobayashi, E.; Kriegler, E.; et al. Mitigation pathways compatible with 1.5 °C in the context of sustainable development. In *Global Warming of 1.5 °C. An IPCC Special Report on the Impacts of Global Warming of 1.5 °C Above Pre-Industrial Levels and Related Global Greenhouse Gas Emission Pathways, in the Context of Strengthening the Global Response to the Threat of Climate Change, Sustainable Development, and Efforts to Eradicate Poverty*; Masson-Delmotte, V.P., Zhai, H.-O., Pörtner, D., Roberts, J., Skea, P.R., Shukla, A., Pirani, W., Moufouma-Okia, C., Péan, R., Pidcock, S., et al., Eds.; 2018; in press.
3. Anderson, T.R.; Hawkins, E.; Jones, F.D. CO_2, the greenhouse effect and global warming: From the pioneering work of arrhenius and callendar to today's earth system models. *Endeavour* **2016**, *3*, 178–187. [CrossRef] [PubMed]
4. Aresta, M.; Nocito, F.; Dibenedetto, A. What catalysis can do for boosting CO_2 utilization. *Adv. Catal.* **2018**, *62*, 49–111.
5. De Souza, A.L.A.; Vieira, M.O.; Polesso, B.B.; Cobalchini, F.W.; Bernard, F.L.; Vecchia, F.D.; Einloft, S. Sorção de CO_2 utilizando líquido iônico aditivado com extensores de área superficial. *Quim. Nova* **2018**, *41*, 656–661. [CrossRef]
6. Meylan, F.D.; Moreau, V.; Erkman, S. CO_2 utilization in the perspective of industrial ecology, an overview. *J. CO_2 Util.* **2015**, *12*, 101–108. [CrossRef]
7. Yang, Z.; He, L.; Gao, J.; Liu, A.; Yu, B. Carbon dioxide utilization with C–N bond formation: Carbon dioxide capture and subsequent conversion. *Energy Environ. Sci.* **2012**, *5*, 6602–6639. [CrossRef]
8. Monteiro, W.F.; Vieira, M.O.; Aquino, A.S.; Souza, M.O.; Lima, J.; Einloft, S.; Ligabue, R. CO_2 conversion to propylene carbonate catalyzed by ionic liquid containing organosilane groups supported on titanate nanotubes/nanowires. *Appl. Catal. A Gen.* **2017**, *544*, 46–54. [CrossRef]
9. Muldoon, M.J.; Aki, S.; Anderson, J.L.; Dixon, J.K.; Brennecke, J.F. Improving carbon dioxide solubility in ionic liquids. *J. Phys. Chem. B* **2007**, *111*, 9001–9009. [CrossRef]

10. Vieira, M.O.; Aquino, A.S.; Schütz, M.K.; Vecchia, F.D.; Ligabue, R.; Seferin, M.; Einloft, S. Chemical conversion of CO_2: Evaluation of different ionic liquids as catalysts in dimethyl carbonate synthesis. *Energy Procedia* **2017**, *114*, 7141–7149. [CrossRef]
11. Aquino, A.S.; Bernard, F.L.; Vieira, M.O.; Borges, J.V.; Rojas, M.F.; Vecchia, F.D.; Ligabue, R.; Seferin, M.; Menezes, S.; Einloft, S. A new approach to CO_2 capture and conversion using imidazolium based-ionic liquids as sorbent and catalyst. *J. Braz. Chem. Soc.* **2014**, *25*, 2251–2257.
12. Vieira, M.O.; Monteiro, W.F.; Neto, B.S.; Ligabue, R.; Chaban, V.V.; Einloft, S. Surface active ionic liquids as catalyst for CO_2 conversion to propylene carbonate. *Catal. Lett.* **2018**, *148*, 108–118. [CrossRef]
13. Vekariya, R.L. A review of ionic liquids: Applications towards catalytic organic transformations. *J. Mol. Liq.* **2017**, *227*, 44–60. [CrossRef]
14. Martinez, A.S.; Hauzenberger, C.; Sahoo, A.R.; Csendes, Z.; Hoffmann, H.; Bica, K. Continuous conversion of carbon dioxide to propylene carbonate with supported ionic liquids. *ACS Sustain. Chem. Eng.* **2018**, *6*, 13131–13139. [CrossRef]
15. Vieira, M.O.; Monteiro, W.F.; Neto, B.S.; Chaban, V.V.; Ligabue, R.; Einloft, S. Chemical fixation of CO_2: The influence of linear amphiphilic anions on surface active ionic liquids (SAILs) as catalysts for synthesis of cyclic carbonates under solvent-free conditions. *React. Kinet. Mech. Cat.* **2019**, *126*, 987–1001. [CrossRef]
16. Ramdin, M.; Amplianitis, A.; de Loos, T.W.; Vlugt, T. Solubility of CO_2/CH_4 gas mixtures in ionic liquids. *Fluid Phase Equilib.* **2014**, *375*, 134–142. [CrossRef]
17. Anderson, J.L.; Dixon, J.K.; Brennecke, J.F. Solubility of CO_2, CH_4, C_2H_6, C_2H_4, O_2, and N_2 in 1-Hexyl-3-methylpyridinium Bis(trifluoromethylsulfonyl)imide: Comparison to other ionic liquids. *Acc. Chem. Res.* **2007**, *40*, 1208–1216. [CrossRef] [PubMed]
18. Ramdin, M.; de Loos, T.W.; Vlugt, T. State of the art of CO_2 capture with ionic liquids. *Ind. Eng. Chem. Res.* **2012**, *51*, 8149–8177. [CrossRef]
19. Corvo, M.C.; Sardinha, J.; Casimiro, T.; Marin, G.; Seferin, M.; Einloft, S.; Menezes, S.; Dupont, J.; Cabrita, E. A rational approach to CO_2 capture by imidazolium ionic liquids: Tuning CO_2 solubility by cation alkyl branching. *ChemSusChem* **2015**, *8*, 1935–1946. [CrossRef] [PubMed]
20. Ma, T.; Wang, J.; Du, Z.; Abdeltawab, A.A.; Al-Enizi, A.M.; Chen, X.; Yu, G. A process simulation study of CO_2 capture by ionic liquids. *Int. J. Greenh. Gas. Contr.* **2017**, *58*, 223–231. [CrossRef]
21. Vieira, M.O.; Monteiro, W.F.; Ligabue, R.; Seferin, M.; Chaban, V.V.; Andreeva, N.A.; Nascimento, J.F.; Einloft, S. Ionic liquids composed of linear amphiphilic anions: Synthesis, physicochemical characterization, hydrophilicity and interaction with carbon dioxide. *J. Mol. Liq.* **2017**, *241*, 64–73. [CrossRef]
22. Rodríguez-Perez, L.; Coppel, Y.; Favier, I.; Teuma, E.; Serp, P.; Gomez, M. Imidazolium-based ionic liquids immobilized on solid supports: Effect on the structure and thermostability. *Dalton Trans.* **2010**, *39*, 7565–7568. [CrossRef] [PubMed]
23. Wan, M.M.; Zhu, H.Y.; Li, Y.Y.; Ma, J.; Liu, S.; Zhu, J.H. Novel CO_2-capture derived from the basic ionic liquids orientated on mesoporous materials. *ACS Appl. Mater. Interfaces* **2014**, *6*, 12947–12955. [CrossRef] [PubMed]
24. Romanos, G.E.; Schulz, P.S.; Bahlmann, M.; Wasserscheid, P.; Sapalidis, A.; Katsaros, F.K.; Athanasekou, C.P.; Beltsios, K.; Kanellopoulos, N.K. CO_2 capture by novel supported ionic liquid phase systems consisting of silica nanoparticles encapsulating aminefunctionalized ionic liquids. *J. Phys. Chem. C* **2014**, *118*, 24437–24451. [CrossRef]
25. Aquino, A.S.; Bernard, F.L.; Borges, J.V.; Mafra, L.; Vecchia, F.D.; Vieira, M.O.; Ligabue, R.; Seferin, M.; Chaban, V.V.; Cabrita, E.; et al. Rationalizing the role of the anion in CO_2 capture and conversion using imidazolium-based ionic liquid modified mesoporous silica. *RSC Adv.* **2015**, *5*, 64220–64227. [CrossRef]
26. Valkenberg, M.H.; Castro, C.; Hölderich, W.F. Immobilisation of ionic liquids on solid supports. *Green Chem.* **2001**, *4*, 88–93. [CrossRef]
27. Luza, L.; Gual, A.; Eberhardt, D.; Teixeira, S.R.; Chiaro, S.; Dupont, J. Imprinting catalytically active Pd nanoparticles onto ionic-liquid-modified Al_2O_3 supports. *Chem. Cat. Chem.* **2013**, *5*, 2471–2478.
28. Karout, A.; Pierre, A.C. Silica xerogels and aerogels synthesized with ionic liquids. *J. Non Cryst. Solids* **2007**, *353*, 2900–2909. [CrossRef]
29. Donato, K.Z.; Donato, R.K.; Lavorgna, M.; Ambrosio, L.; Matejka, L.; Mauler, R.S.; Schrekker, H.S. Ionic liquids as dynamic templating agents for sol–gel silica systems: Synergistic anion and cation effect on the silica structured growth. *J. Sol Gel Sci Technol.* **2015**, *76*, 414–427. [CrossRef]

30. Rahman, I.A.; Padavettan, V. Synthesis of silica nanoparticles by sol–gel: Size-dependent properties, surfacemodification, and applications in silica-polymer nanocomposites—A review. *J. Nanomater.* **2012**, *8*, 1–15. [CrossRef]
31. Zhang, J.; Ma, Y.; Shi, F.; Liu, L.; Deng, Y. Room temperature ionic liquids as templates in the synthesis of mesoporous silica via a sol–gel method. *Microporous Mesoporous Mater.* **2009**, *119*, 97–103. [CrossRef]
32. Romanovsky, B.V.; Tarkhanova, I.G. Supported ionic liquids in catalysis. *Rus. Chem. Rev.* **2017**, *86*, 444–458. [CrossRef]
33. Vioux, A.; Viau, L.; Volland, S.; Bideau, J.L. Use of ionic liquids in sol–gel; ionogels and applications. *C. R. Chimie* **2010**, *13*, 242–255. [CrossRef]
34. Mitra, S.; Cerclier, C.; Berrod, Q.; Ferdeghini, F.; de Oliveira-Silva, R.; Judeinstein, P.; Bideau, J.; Zanotti, J. Ionic liquids confined in silica ionogels: Structural, thermal, and dynamical behaviors. *Entropy* **2017**, *19*, 140. [CrossRef]
35. Vidinha, P.; Barreiros, S.; Cabral, J.M.S.; Nunes, T.G.; Fidalgo, A.; Ilharco, L.M. Enhanced biocatalytic activity of ORMOSIL-encapsulated cutinase: The matrix structural perspective. *J. Phys. Chem. C* **2008**, *112*, 2008–2015. [CrossRef]
36. Karimi, B.; Enders, D. New N-heterocyclic carbene palladium complex/ionic liquid matrix immobilized on silica: Application as recoverable catalyst for the heck reaction. *Org. Lett.* **2006**, *8*, 1237–1240. [CrossRef] [PubMed]
37. Lesniewski, A.; Niedziolka, J.; Palys, B.; Rizzi, C.; Gaillon, L.; Opallo, M. Electrode modified with ionic liquid covalently bonded to silicate matrix for accumulation of electroactive anions. *Electrochem. Commun.* **2007**, *9*, 2580–2584. [CrossRef]
38. Amini, R.; Rouhollahi, A.; Adibi, M.; Mehdinia, A. A novel reusable ionic liquid chemically bonded fused-silica fiber for headspace solid-phase microextraction/gas chromatography-flame ionization detection of methyl tert-butyl ether in a gasoline sample. *J. Chromatogr. A* **2011**, *1218*, 130–136. [CrossRef] [PubMed]
39. Dreisbach, F.; Lösch, H.W. Highest pressure adsorption equilibria data: Measurement with magnetic suspension balance and analysis with a new adsorbent/adsorbate-volume. *Adsorption* **2002**, *8*, 95–109. [CrossRef]
40. Belmabkhout, Y.; Serna-Guerrero, R.; Sayari, A. Adsorption of CO_2 from dry gases on MCM-41 silica at ambient temperature and high pressure. 1: Pure CO2 adsorption. *Chem. Eng. Sci.* **2009**, *64*, 3721–3728. [CrossRef]
41. Paschoal, V.H.; Faria, L.F.O.; Ribeiro, M.C.C. Vibrational Spectroscopy of Ionic Liquids. *Chem. Rev.* **2017**, *117*, 7053–7112. [CrossRef] [PubMed]
42. Galgano, P.D.; El Seoud, O.A. Surface active ionic liquids: Study of the micellar properties of 1-(1-alkyl)-3-methylimidazolium chlorides and comparison with structurally related surfactants. *J. Coll. Interface Sci.* **2011**, *361*, 186–194. [CrossRef] [PubMed]
43. Jadhav, P.D.; Chatti, R.V.; Biniwale, R.B.; Labhsetwar, N.K.; Devotta, S.; Rayalu, S.S. Monoethanol amine modified zeolite 13X for CO_2 adsorption at different temperatures. *Energ. Fuels* **2007**, *21*, 3555–3559. [CrossRef]
44. Xu, X.; Zhao, X.; Sun, L.; Liu, X. Adsorption separation of carbon dioxide, methane and nitrogen on monoethanol amine modified β-zeolite. *J. Nat. Gas Chem.* **2009**, *18*, 167–172. [CrossRef]